

Reionizing the Universe in Warm Dark Matter cosmologies

Pratika Dayal^{1,2*}, Tirthankar Roy Choudhury³, Volker Bromm⁴ & Fabio Pacucci⁵

¹ *SUPA†, Institute for Astronomy, University of Edinburgh, Royal Observatory, Edinburgh, EH9 3HJ, UK*

² *Institute for Computational Cosmology, Department of Physics, University of Durham, South Road, Durham DH1 3LE, UK*

³ *National Centre for Radio Astrophysics, Tata Institute of Fundamental Research, Pune 411007, India*

⁴ *Department of Astronomy and Texas Cosmology Centre, University of Texas, Austin, TX 78712, USA*

⁵ *Scuola Normale Superiore, Piazza dei Cavalieri 7, 56126 Pisa, Italy*

ABSTRACT

We compare model results from our semi-analytic merger tree based framework for high-redshift ($z \simeq 5 - 20$) galaxy formation against reionization indicators including the *Planck* electron scattering optical depth (τ_{es}) and the ionizing photon emissivity (\dot{n}_{ion}) to constrain the particle mass of Warm Dark Matter (WDM). Our framework traces the Dark Matter (DM) and baryonic assembly of galaxies in 4 DM cosmologies: Cold Dark Matter (CDM) and WDM with a particle mass of $m_x = 2.25, 3$ and 5 keV. It includes all the key processes of star formation, supernova feedback, the merger/accretion/ejection driven evolution of gas and stellar mass, and the effect of the ultra-violet background (UVB) created during reionization in photo-evaporating the gas content of galaxies in halos with $M_h \lesssim 10^9 M_\odot$. We show that current *Planck* τ_{es} values rule out $m_x \lesssim 2.5$ keV WDM, even in the physically unlikely scenario that all ionizing photons produced by these galaxies escape and contribute to reionization (i.e. $f_{esc} = 1$). With the largest number of UVB-suppressed galaxies, CDM faces a “stalling” of the reionization process with this effect decreasing with the disappearance of small-scale structure with decreasing m_x . Finally, we find the bulk of the reionization photons come from galaxies with a halo mass $M_h \lesssim 10^9 M_\odot$, stellar mass $M_* \lesssim 10^7 M_\odot$ and UV magnitude $-18 \lesssim M_{UV} \lesssim -13$ in CDM. The progressive suppression of low-mass halos with decreasing m_x leads to a shift in the “reionization” population to larger (halo and stellar) masses of $M_h \gtrsim 10^9 M_\odot$ and $M_* \gtrsim 10^7 M_\odot$ for $m_x \gtrsim 3$ keV WDM, although the UV limits effectively remain unchanged.

Key words: Cosmology:dark matter-reionization-cosmological parameters-cosmic microwave background; galaxies-intergalactic medium

1 INTRODUCTION

According to the standard Lambda Cold Dark Matter (Λ CDM) cosmological model, galaxy formation proceeds hierarchically through time, driven by a cold (dark) matter of unknown composition. In this era of precision cosmology, its energy density has been measured to have a value of $\Omega_m h^2 = 0.133$ with baryons comprising $\Omega_b h^2 = 0.0196$ of the total (Planck Collaboration et al. 2014b). CDM clusters on all scales and has been remarkably successful in predicting the large scale structure of the Universe, the temperature anisotropies measured by the Cosmic Microwave Background (CMB) and Lyman- α forest statistics (e.g. Peebles

1971; Blumenthal et al. 1984; Bond & Szalay 1983; Cole et al. 2005; Lange et al. 2001; Hinshaw et al. 2013; Planck Collaboration et al. 2014a; Slosar et al. 2013). However, as recently reviewed by Weinberg et al. (2013), CDM exhibits a number of small scales problems: it produces halo profiles that are cuspy as opposed to the observationally preferred constant density cores (Navarro et al. 1997; Subramanian et al. 2000), it over-predicts the number of satellite and field galaxies as compared to observations (the “missing satellite problem”; Klypin et al. 1999; Moore et al. 1999), predicts massive (Large Magellanic Cloud mass), concentrated Galactic subhalos inconsistent with observations (e.g. Boylan-Kolchin et al. 2012) and faces difficulty in producing typical disks due to ongoing mergers down to $z \simeq 1$ (Wyse 2001). The limited success of baryonic feedback in solving these small scale problems (e.g. Boylan-Kolchin et al. 2012;

* prd@roe.ac.uk

† Scottish Universities Physics Alliance

Teyssier et al. 2013) has prompted questions regarding the validity of the CDM scenario. A popular solution to the small scale problems in CDM cosmology involves invoking (\sim keV) Warm Dark Matter (WDM) particles that erase small-scale power (Blumenthal et al. 1984; Bode et al. 2001, e.g.)¹. Beyond its Standard Model, particle physics provides compelling motivation for WDM candidates, which can be as light as $\sim \mathcal{O}(1)$ KeV, such as sterile neutrinos. These appear in an extension of the Standard Model with 3 sterile neutrinos, out of which 2 could be as heavy as $1 - 10$ GeV, while the lightest one could be within $\mathcal{O}(1)$ keV (for a review see Abazajian et al. 2012). There are some tantalising observational hints such as the 3.5 keV monochromatic line observed by XMM-Newton coming from the Perseus galaxy cluster. This line might arise from a light sterile neutrino annihilating into photons (Bulbul et al. 2014; Boyarsky et al. 2014).

Astrophysical constraints on the WDM particle mass range from $m_x \geq 3.3$ keV using the Ly α forest power spectrum (Viel et al. 2013), $m_x > 1.6 - 1.8$ keV using number counts of high- z gamma ray bursts (de Souza et al. 2013), $m_x \gtrsim 1.3$ keV using abundance matching of theoretical and observed high- z galaxies (Schultz et al. 2014), $m_x \gtrsim 1$ keV using dwarf spheroidal galaxy observations (de Vega & Sanchez 2010), simultaneously reproducing stellar mass functions and the Tully-Fisher relation for $z = 0 - 3.5$ galaxies (Kang et al. 2013) and comparing the observed number density of $z \approx 10$ galaxies to that expected from the halo mass function (Pacucci et al. 2013), and $m_x \gtrsim 0.5$ keV inferred using the presence of supermassive black holes at $z \simeq 5.8$ (Barkana et al. 2001),

A combination of ground and space-based observations has allowed a statistically significant data available for $z \simeq 6 - 10$ Lyman Break galaxies (LBGs; Oesch et al. 2010; Bouwens et al. 2010, 2011; Castellano et al. 2010; McLure et al. 2010; Bradley et al. 2012; Oesch et al. 2013; McLure et al. 2013; Bowler et al. 2014b; Bouwens et al. 2014; Bowler et al. 2014a) enabling such constraints to be extended to the high- z Universe. Indeed, in Dayal et al. (2014b), we presented a merger-tree based semi-analytic model that traces both the DM and baryonic assembly of high- z ($z \simeq 7 - 15$) galaxies in 4 cosmologies: CDM and WDM with particle masses $m_x = 1.5, 3$ and 5 keV. While the halo mass function is indistinguishable for CDM and $m_x \gtrsim 3$ keV WDM down to halo masses as low as $M_h \simeq 10^{8.5} M_\odot$, small mass ($M_h \simeq 10^{9.5} M_\odot$) structures are suppressed more severely in the 1.5 keV scenario. We showed that the ultraviolet luminosity functions (UV LFs), mass to light (M/L ratios) and stellar mass densities (SMD) are the same in all the 4 models for the massive, luminous ($M_{UV} \leq -18$) galaxies that have been observed so far. However, the delay in structure formation in the 1.5 keV WDM scenario leads to a delayed and accelerated baryonic assembly resulting in a steeper SMD

¹ However, some works caution that the extremely low mass WDM particles required to make constant density cores prevent the very formation of dwarf galaxies (Macciò et al. 2012; Schneider et al. 2014).

evolution with redshift, that should be detectable by the *James Webb Space Telescope* (JWST) integrating down to $M_{UV} \simeq -16.5$ at $z \gtrsim 10$ (see also Calura et al. 2014; Governato et al. 2014).

Since low-mass high- z galaxies are now believed to be the main sources of reionization photons in the early Universe (e.g. Barkana & Loeb 2001; Ciardi & Ferrara 2005; Choudhury & Ferrara 2007; Choudhury et al. 2008), their delayed and accelerated assembly would naturally lead to a corresponding delay and acceleration in the reionization history. Now that we have verified that our theoretical galaxy populations are in agreement with observations at $z \simeq 7 - 12$ for $m_x = 1.5, 3$ and 5 keV, we build reionization histories for 4 DM models with $m_x = 2.25, 3$ and 5 keV to see if we can obtain tighter constraints on m_x by comparing to existing observations of the *Planck* CMB electron scattering optical depth and the ionizing photon emissivity. In addition to internal feedback from supernovae (see Sec. 2.3 Dayal et al. 2014b) our model self-consistently includes the “external” feedback effect from reionization in photo-evaporating gas from DM halos (Sec. 2.2), and yields both the reionization history, and the ionizing photon contribution across different halo mass, stellar mass and magnitude bins (Sec. 3), as explained in what follows.

The cosmological parameters used in this work correspond to $(\Omega_m, \Omega_\Lambda, \Omega_b, h, n_s, \sigma_8) = (0.2725, 0.702, 0.04, 0.7, 0.96, 0.83)$, consistent with the latest results from the *Planck* collaboration (Planck Collaboration et al. 2014b) and we quote all quantities in comoving units unless stated otherwise.

2 THEORETICAL MODEL

We now briefly summarise the theoretical model and interested readers are referred to Dayal et al. (2014a,b) for complete details. We explore 4 DM models: CDM and WDM with $m_x = 2.25, 3$ and 5 keV. Although we cite m_x values assuming thermally decoupled relativistic particles, these numbers can also be converted into sterile neutrino masses ($m_{sterile \nu}$) using (Viel et al. 2005)

$$m_{sterile \nu} = 4.43 \text{ keV} \left(\frac{m_x}{1 \text{ keV}} \right)^{4/3} \left(\frac{0.1225}{\Omega_m h^2} \right), \quad (1)$$

yielding $m_{sterile \nu} = (13.1, 18.6, 36.8) \text{ keV}$ corresponding to $m_x = (2.25, 3, 5) \text{ keV}$ respectively.

2.1 Merger trees and the baryonic implementation

We start by constructing 400 merger trees starting at $z = 4$ linearly distributed across the halo mass range $\log(M_h/M_\odot) = 9 - 13$ for the 4 DM models considered. The merger-trees use 320 equal redshift steps ($\Delta z = 0.05$) between $z = 20$ and $z = 4$ with a mass resolution of $M_{res} = 10^8 M_\odot$ using the modified binary merger tree algorithm with smooth accretion detailed in Parkinson et al.

(2008) and Benson et al. (2013). We scale the relative abundances of the merger tree roots to match the $z = 4$ Sheth-Tormen halo mass function (HMFs; Sheth & Tormen 1999) and have verified that these yield HMFs in good agreement with the Sheth-Tormen (Sheth & Tormen 1999) HMF at all z .

We implement the merger trees with baryonic physics including star formation, supernova (SN) feedback driven ejection of gas, and the merger/accretion/ejection driven evolution of the gas and stellar masses. Our model is based on the simple premise that the maximum star formation efficiency (f_*^{eff}) of any halo is limited by the SN binding energy required to unbind/eject the rest of the gas and quench further star formation, up to a maximum threshold value of f_* (see Dayal et al. 2014a). This model has two z and mass independent free parameters whose values are selected to match the evolving UV LF: the maximum threshold star formation efficiency (f_*) and the fraction of SN energy that goes into unbinding gas (f_w). While f_w affects the faint-end slope of the UV LF where feedback is most effective, f_* determines the normalization at the bright-end where galaxies can form stars with the maximum allowed efficiency.

We implement this simple idea proceeding forward in time from the highest merger tree output redshift, $z = 20$. At any z step, the initial gas mass, $M_{g,i}(z)$, in a galaxy depends on its merger history: while galaxies that have no progenitors are assigned a value $M_{g,i}(z) = (\Omega_b/\Omega_m)M_h(z)$, the value is determined both by the gas mass brought in by merging progenitors as well as that smoothly-accreted from the intergalactic medium (IGM) for galaxies that have progenitors. A part (f_*^{eff}) of this gas forms new stellar mass, $M_*(z)$ with the final gas mass left depending on the ratio of the (instantaneous) energy provided by exploding SN and the potential energy of the halo. We note that at any step, the total stellar mass in a galaxy is the sum of mass of the newly-formed stars, and that brought in by its progenitors.

For simplicity, we assume every new stellar population has a fixed metallicity of $0.05Z_\odot$ and an age $t_0 = 2$ Myr. Using the population synthesis code STARBURST99 (Leitherer et al. 1999), its initial UV luminosity (at $\lambda = 1500$ Å) can be calculated as $L_{UV}(0) = 10^{33.077}(M_*/M_\odot) \text{ erg s}^{-1} \text{ Å}^{-1}$ and the initial output of ionizing photons can be calculated as $\dot{N}_{ion}(0) = 10^{46.6255}(M_*/M_\odot) \text{ s}^{-1}$. Further, the time evolution of these quantities can be expressed as

$$L_{UV}(t) = L_{UV}(0) - 1.33 \log \frac{t}{t_0} + 0.462 \quad (2)$$

$$\dot{N}_{ion}(t) = \dot{N}_{ion}(0) - 3.92 \log \frac{t}{t_0} + 0.7 \quad (3)$$

For any galaxy along the merger tree, its UV luminosity and ionizing photon output rate are the sum of the values from the new starburst, and the contribution from older populations accounting for the drop with time. We therefore have these quantities for 320 z steps between $z = 20$ and $z = 4$.

As shown in Dayal et al. (2014a,b), our model reproduces the observed UV LF for all DM models (CDM and WDM with $m_x = 1.5, 3$ and 5 keV) at $z \simeq 5 - 10$ over 2.5 orders of magnitude in luminosity (7 magnitudes in M_{UV})

and predicts the z -evolution of the faint end UV LF slope in addition to reproducing observables including the SMD and mass-to-light ratios using fiducial parameter values of $f_* = 0.038$ and $f_w = 0.1$. We maintain these fiducial parameter values in all the calculations carried out in this work. Further, we replace 1.5 keV WDM with a heavier mass of 2.25 keV to get tighter constraints on m_x ; we note that the latter mass naturally fits all of the observed data sets presented in Dayal et al. (2014a,b).

2.2 Modelling reionization

The quantity which plays a crucial role in modelling reionization is the rate of ionizing photons per unit comoving volume \dot{n}_{ion} ($\text{s}^{-1} \text{ Mpc}^{-3}$) in the IGM, which is essentially obtained by (i) integrating the photon production rate \dot{N}_{ion} of individual galaxies over relevant halo mass ranges, and (ii) multiplying by the fraction f_{esc} of ionizing photons that escape from halos into the IGM.

Although reionization is driven by the H I ionizing photons produced by early galaxies, the ultra-violet background (UVB) built up during reionization suppresses the baryonic content of galaxies by photo-heating/evaporating gas at their outskirts (Klypin et al. 1999; Moore et al. 1999; Somerville 2002) preventing efficient cooling and slowing down its progress. In order to account for the effect of reionization feedback on \dot{n}_{ion} , we assume total photo-evaporation of gas from halos below $M_{min} = 10^9 M_\odot$ (at any z) within ionized regions. In other words, halos below M_{min} and can neither form stars nor contribute any gas in mergers if they are forming inside the regions which have already been ionized. Hence the globally averaged \dot{n}_{ion} is given by

$$\dot{n}_{ion}(z) = f_{esc}(z)[Q_{II}(z)\dot{n}_{II}(z) + [1 - Q_{II}(z)]\dot{n}_I(z)], \quad (4)$$

where $Q_{II}(z)$ is the volume filling fraction for ionized regions, and \dot{n}_{II} (\dot{n}_I) is the photon production rate density within ionized (neutral) regions. Clearly \dot{n}_I contains contribution from all sources which can form stars and is unaffected by the UVB, while \dot{n}_{II} represents the case where sources below M_{min} do not contribute to ionizing photons. At the beginning of the reionization process the volume filled by ionized hydrogen is very small ($Q_{II} \ll 1$) and most galaxies are not affected by the UVB, thus giving $\dot{n}_{ion}(z) \approx \dot{n}_I(z)$. However, as Q_{II} increases and reaches a value $\simeq 1$ (note reionization is said to be complete when $Q_{II} = 1$), all galaxies less massive than M_{min} are feedback-suppressed such that $\dot{n}_{ion}(z) \approx \dot{n}_{II}(z)$.

The reionization history, expressed through the evolution of Q_{II} , can then be written as

$$\frac{dQ_{II}}{dz} = \frac{dn_{ion}}{dz} - \frac{Q_{II}}{t_{rec}} \frac{dt}{dz}, \quad (5)$$

where $dt/dz = [H(z)(1+z)]^{-1}$. Here, the first term on the right hand side represents the ionizing photon production which drives reionization, and the second term shows the decrease in the H II volume filling fraction due to recombination of electrons and protons to form H I. Further, n_H is the comoving hydrogen number density, and t_{rec} is the recombination time that can be expressed as

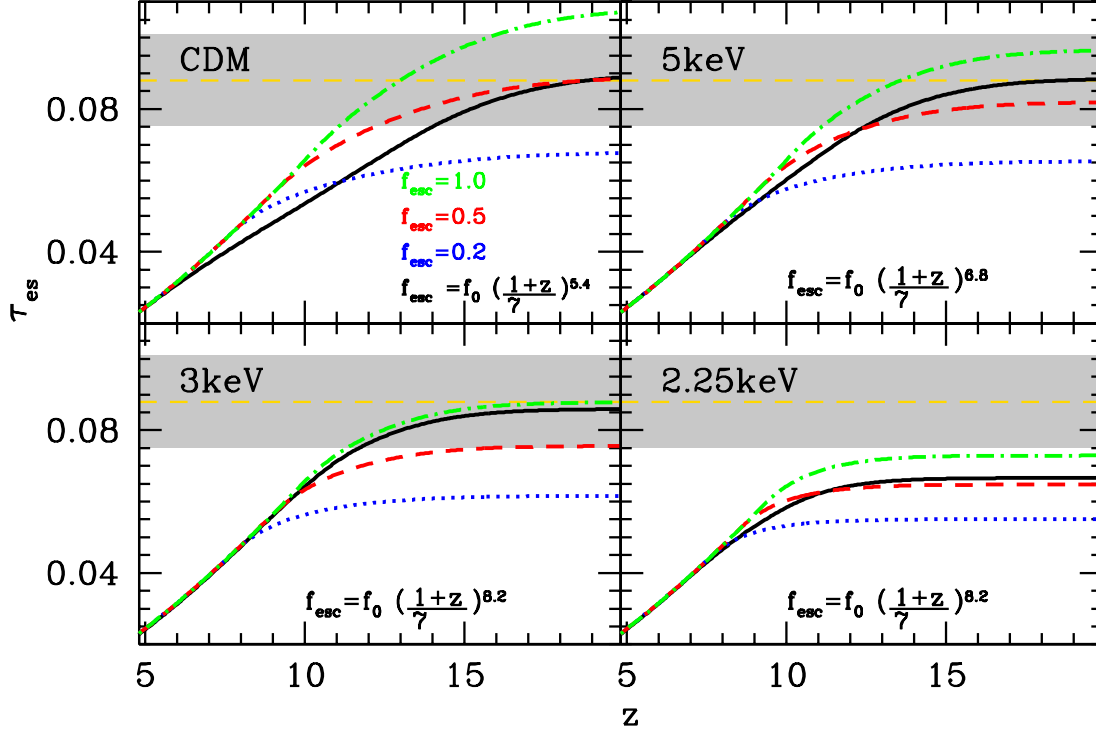


Figure 1. The CMB electron scattering optical depth (τ_{es}) as a function of redshift for the 4 DM models considered in this paper, as marked in each panel. In each panel, the 4 lines show results using four different values of $f_{esc} = 1.0$ (dot-dashed line), 0.5 (dashed line), 0.35 (dotted line) and the fiducial z -dependent value marked (solid line); we use the same z -dependence of f_{esc} for both the 3 and 2.25 keV cases. The z -dependent f_{esc} value has been obtained by simultaneously fitting to τ_{es} and ionizing photon emissivity observations. The horizontal dashed line shows the central value for τ_{es} inferred by *Planck* with the shaded region showing the errors allowed (Planck Collaboration et al. 2014b). As seen, while a z -dependent f_{esc} gives reasonable results for CDM and $m_x \gtrsim 3$ keV WDM, the 2.25 keV model is effectively ruled out by current CMB constraints, even using the maximum allowed value of $f_{esc} = 1$.

$$t_{rec} = \frac{1}{\chi n_H (1+z)^3 \alpha_B C} \quad (6)$$

where α_B is the hydrogen case-B recombination coefficient, $\chi = 1.08$ accounts for the excess free electrons arising from singly ionized helium and C is the IGM clumping factor which we assume to be evolving as (Pawlik et al. 2009; Haardt & Madau 2012)

$$C = \frac{\langle n_{HII}^2 \rangle}{\langle n_{HII} \rangle^2} = 1 + 43 z^{-1.71}. \quad (7)$$

As seen above, the photon production rate depends on f_{esc} and hence we need to know the value of the parameter to calculate the reionization history. In this work we assume f_{esc} to be independent of the halo mass, and take to be a function of only z . Once the function $f_{esc}(z)$ is chosen, the reionization history of the model can be worked out. As shown in Sec. 3.1 that follows, simultaneously fitting to observations of the CMB electron scattering optical depth (τ_{es}) and the ionizing emissivity (\dot{n}_{ion}) require a z -dependent f_{esc} that evolves as

$$f_{esc} = f_0 \left(\frac{1+z}{7} \right)^\alpha, \quad (8)$$

where f_0 and α are z -independent parameters whose values for different DM models are shown in Table 1.

3 RESULTS

Now that the model has been described we start by discussing the model constraints on m_x using observed values of the CMB electron scattering optical depth (τ_{es}) and ionizing emissivity (\dot{n}_{ion}). We then present the inferred reionization history and sources for all the 4 DM models, as described in what follows.

3.1 Joint reionization constraints from the CMB optical depth and UVB emissivity

Combining *Planck* and *WMAP* low- l polarization data, the current best estimate of $\tau_{es} = 0.089^{+0.012}_{-0.014}$ (Planck Collaboration et al. 2014b). We calculate τ_{es} at any given z by solving the equation:

$$\tau_{es}(z) = \sigma_T C \int_0^z dt n_e (1+z)^3 \quad (9)$$

where $n_e(z) = Q_{II}(z)n_H$ is the global average comoving value of the electron number density and $\sigma_T = 6.6524 \times$

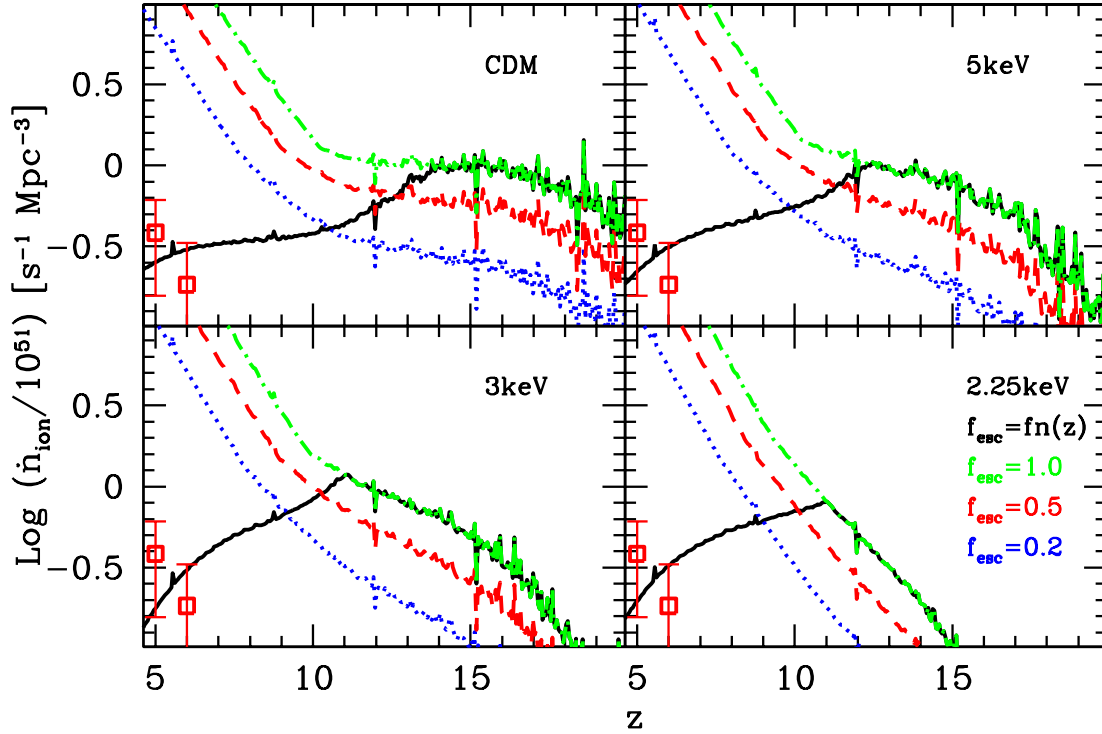


Figure 2. Redshift evolution of the H I ionizing photon emissivity (for all theoretical galaxies) for the 4 DM models considered in this paper, as marked in each panel. In each panel, the 4 lines show results using four different values of $f_{esc} = 1.0$ (dot-dashed line), 0.5 (dashed line), 0.35 (dotted line) and the fiducial z -dependent value (solid line); we use the same z -dependence of f_{esc} for both the 3 and 2.25 keV cases. As clearly seen, a constant f_{esc} value severely over-predicts \dot{n}_{ion} compared to the observations (points) at $z \simeq 5, 6$ in all DM models. The observational results (and associated error bars) have been calculated following the approach of Kuhlen & Faucher-Giguere (2012), i.e., by combining the observational constraints on Γ_{HI} from Wyithe & Bolton (2011) with λ_{mfp} from Songaila & Cowie (2010). See text for details.

Model	$f_0 \times 100$	α
CDM	1.65	5.4
$m_x = 5$ keV (13.1 keV)	1.25	6.8
$m_x = 3$ keV (18.6 keV)	1.2	8.2
$m_x = 2.25$ keV (36.8 keV)	1.2	8.2

Table 1. The parameter values for z -evolution of the escape fraction f_{esc} for different DM models; the numbers in brackets show the sterile neutrino mass corresponding to m_x . The z -dependence of f_{esc} is taken to be $f_{esc}(z) = f_0[(1+z)/7]^\alpha$.

10^{-25} cm^2 is the Thomson scattering cross-section. Note that f_{esc} governs the evolution of Q_{II} as shown in Eqns. 4 and 5.

A second observable that needs to be fit by any reionization model is the emissivity of ionizing photons at $z \lesssim 6$. It is currently believed that reionization was completed in a “photon-starved” manner, which is constrained mainly by the observations of H I photoionization rate Γ_{HI} from quasar absorption lines (Ly α forest) at $5 \leq z \leq 6$ (Bolton & Haehnelt 2007). In order to calculate Γ_{HI} in reionization models, one needs to model the mean free path λ_{mfp} of ion-

izing photons in addition to \dot{n}_{ion} (see, e.g., Choudhury & Ferrara 2005, 2006). In this work, we follow the approach of Kuhlen & Faucher-Giguere (2012) and combine the observational constraints on Γ_{HI} from Wyithe & Bolton (2011) with λ_{mfp} from Songaila & Cowie (2010) to obtain the observational estimate of \dot{n}_{ion} . We have used the fiducial values from Kuhlen & Faucher-Giguere (2012): $\gamma = 1$ for the source spectral index and $\beta = 1.3$ for the H I column density distribution. Varying these within allowed would only result in larger error bars, hence leaving our results unchanged (see Kuhlen & Faucher-Giguere 2012).

The most common approach adopted in calculating the reionization history (and τ_{es}) is to assume a redshift-independent constant value of f_{esc} (e.g. Schultz et al. 2014). We start by following this basic approach to calculate τ_{es} and \dot{n}_{ion} for our 4 DM models, to compare to observations. As shown in Fig. 1, matching to the *Planck* optical depth constraints requires $f_{esc} \gtrsim 0.5$ for CDM and $m_x \gtrsim 3$ keV WDM models; a value of $f_{esc} = 0.2$ does not result in enough electrons to produce the measured optical depth at high- z . As shown in Dayal et al. (2014b, see Fig. 3), structure formation is progressively delayed with decreasing m_x , resulting in a lack of H I ionizing photons which naturally leads to a low value of τ_{es} . Indeed, our model shows that

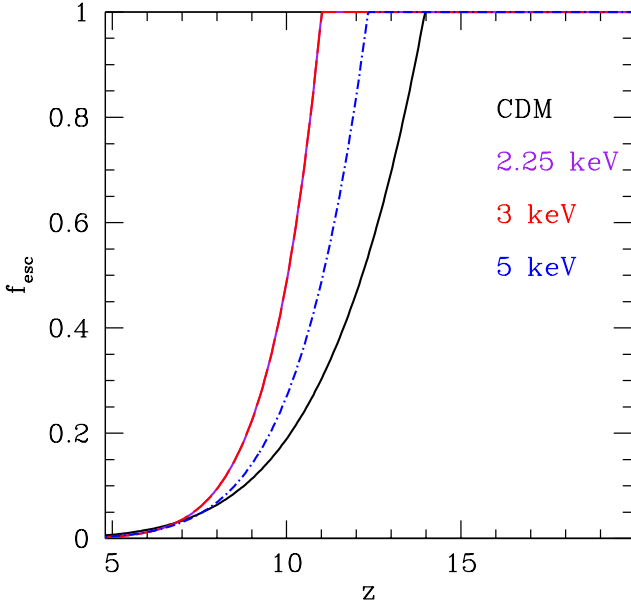


Figure 3. The redshift evolution of the fiducial value of $f_{esc} = f_0(\frac{1+z}{7})^\alpha$ used in this work (see text for details). The results for 2.25 and 3 keV are the same since we use the same z -dependence for both. As seen, progressively lighter WDM particles require a larger photon escape fraction at earlier times to compensate for the lack of low mass halos.

τ_{es} is lower than the *Planck* limits even in the case that $f_{esc} = 1$, where all the H I ionizing photons escape out of galaxies and contribute to reionization *ruling out WDM with $m_x \lesssim 2.25$ keV.*² Although they match the observed τ_{es} , z -independent constant values of $f_{esc} = 0.5(1)$ severely overpredict the ionizing photon emissivity by about 1.6 (1.9) orders of magnitude at $z \simeq 6$ as shown in Fig. 2. A scenario wherein f_{esc} is z -independent is therefore ruled out by the emissivity constraints, irrespective of the DM model considered.

Reconciling these two data sets requires a z -dependent $f_{esc} = f_0[(1+z)/7]^\alpha$ with $\alpha > 0$, which provides enough photons at high- z to obtain the right optical depth τ_{es} , whilst yielding reasonably low \dot{n}_{ion} values at later times; we choose f_0 and α for each DM model such that both the constraints are satisfied simultaneously. The fact that one requires ionizing sources with higher efficiency to match the two data sets has been noted earlier (see e.g., Mitra et al. 2011, 2012). With respect to CDM, the number density of the (low mass) galaxies occupying the faint end of the UV LF ($M_{UV} \gtrsim -11$) is increasingly suppressed with redshift as the WDM particle mass decreases from 5 to 3 keV. This must be compensated

by an increase in f_{esc} (or α) to obtain the required τ_{es} at early epochs: the values of f_0 and α which best fit the central τ_{es} value, while being within \dot{n}_{ion} bounds, for different DM models are shown in Table 1. Given that even the maximum allowed value of $f_{esc} = 1$ is not enough to reach the measured τ_{es} for the 2.25 keV WDM scenario, we simply use the values as in the 3 keV case.³

We show the redshift evolution of the best-fit f_{esc} values for all the DM models in Fig. 3. As mentioned, with the largest number of low mass halos available to provide H I ionizing photons CDM requires a shallower z -dependence on f_{esc} . A successive decrease in the number of low mass halos from CDM to 5 to 3 keV requires a larger f_{esc} at early times, resulting in a steeper z -dependence. To quantify, we find $f_{esc} \simeq 1.4\%$ at $z \simeq 6$ which rises to 50% at $z \simeq 12, 11, 10$ for CDM, 5 and 3 keV WDM, respectively.

3.2 Reionization histories and sources in different DM models

As discussed in Secs. 2.2 and 3.1, given the source galaxy population, the reionization history (or the global z -evolution of Q_{II}) is fixed once the z -evolution of f_{esc} is determined. We start by noting that CDM allows galaxy formation on the smallest scales, with low mass galaxies being progressively suppressed as m_x decreases. It naturally follows that low-mass galaxies in the CDM model will be the most affected by UVB feedback, drawing out the process of reionization with this effect decreasing with the WDM particle mass. This is the behaviour shown in Fig. 4: reionization starts earliest in the CDM model and is 50% complete by $z \simeq 13$, initially driven by low mass halos (see also Bromm & Yoshida 2011). Suppression of star formation in the numerous sources with $M_h \lesssim 10^9 M_\odot$ leads to a “stalling” of the reionization process with only a 10% change in Q_{II} over the 200 Myrs till $z \simeq 9$. Thereafter reionization extends for about 650 Myrs driven by more massive galaxies, with the entire volume being reionized by $z \simeq 5$.

From the same figure we see that while reionization starts off at a slower rate for $m_x = 5$ and 3 keV WDM, it “catches up” fairly quickly due to the slower z -decline of f_{esc} that results in a larger number of ionizing photons; indeed, the IGM is 50% by $z \simeq 11.5 - 12.5$ in these models. As expected, the progressive lack of low-mass galaxies means there is a slightly (almost no) stalling of the reionization process in the 5(3) keV WDM scenario resulting in a quicker end to reionization: indeed, reionization is over by a $z \simeq 6$ (8.5) in the 5(3) keV WDM scenario, having taken

² Note, however, that the constraints on τ_{es} from the recent (12/2014) *Planck* data seem to have been (tentatively) revised to $\tau_{es} = 0.079 \pm 0.017$, see <http://www.cosmos.esa.int/web/planck/ferrara2014> for details. In that case one may be able to reconcile the $m_x = 2.25$ keV case with CMB data by choosing $f_{esc} \gtrsim 0.3$ which yields $\tau_{es} \gtrsim 0.062$.

³ It is, however, possible to obtain a $\tau_{es} \gtrsim 0.062$ for the $m_x = 2.25$ keV case, while at the same time match the \dot{n}_{ion} constraints at $z = 6$, if we choose $f_0 = 1.2$ and $\alpha = 8.2$. These would then be consistent with the latest (12/2014) *Planck* results. We also find that the $m_x = 1.5$ keV WDM gives $\tau_{es} \sim 0.062$ in the unlikely scenario that constant $f_{esc} = 1$, i.e., the new *Planck* results would possibly weaken the lower limit on m_x from 2.25 keV to 1.5 keV if we assumed every ionizing photon produced by 1.5 keV galaxies to have contributed to reionization.

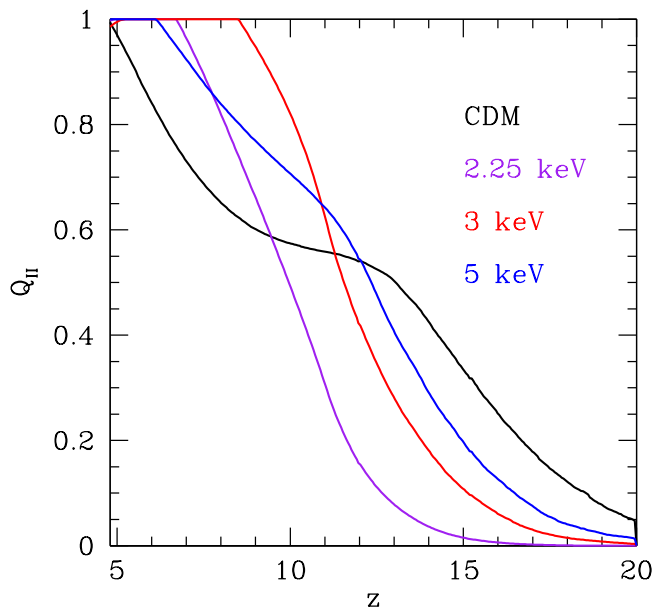


Figure 4. Volume filling fraction of ionized hydrogen as a function of z for the 4 DM models considered using the fiducial model. As seen, reionization is progressively delayed (and its rate enhanced) for decreasing m_x when compared to CDM due to progressive suppression of small scale structure. This naturally results in reionization being the most “drawn-out” for CDM where the effects of the UVB are felt most strongly.

roughly 780 (420) Myrs, as compared to CDM which requires about 1.02 Gyrs. A delay of about a few tens to a 100 Myrs in structure formation results in reionization starting at a $z \simeq 16.5$ in the 2.25 keV WDM scenario. The larger halo masses result in this model being independent of the feedback effects of reionization, resulting in a smooth z -evolution of Q_{II} from completely neutral to ionized in the 520 Myrs between $z \simeq 16.5$ to 6.7. In principle, these different scenarios could be distinguished with future 21cm cosmology surveys with next-generation facilities such as the *Square Kilometre Array (SKA)*.

The next question that needs to be answered concerns the main reionization sources in these 4 DM models, for which we calculate the fractional contribution to the total ionizing emissivity at $z \simeq 5$ from galaxies in varying halo mass, stellar mass and UV magnitude bins as shown in Fig. 5. Starting with the halo mass (panel a), we find that CDM galaxies with $M_h \gtrsim 10^9 M_\odot$ provide only about 35% of the total ionizing photons, with the dominant contribution coming from lower halo masses. As noted, small mass halos are increasingly suppressed with decreasing m_x in WDM models which leads to an increase in the fractional contribution of $M_h \gtrsim 10^9 M_\odot$ galaxies. Indeed, their contribution increases from 50 to 63 to a 80%, as m_x decreases from 5 to 3 to 2.25 keV. As expected from the decreasing number densities with increasing M_h , the contribution of $M_h \gtrsim 10^{10} M_\odot$ halos is lower ($\sim 4\%$ for CDM) and shows the same trend of increasing with decreasing m_x , to $\sim 15\%$ for the 2.25 keV model; this implies galaxies with $M_h \simeq 10^{9-10.5} M_\odot$ pro-

vide about 30% (65%) of the total ionizing photons in CDM (2.25 keV WDM). From the same panel, we see that the UV suppression of low mass halos leads to a flattening in their fractional contribution for CDM. However, the fractional contribution of low mass halos rises much more steeply with decreasing m_x since halos collapse at scales larger than that affected by the UVB.

We now express the fractional contribution of galaxies in terms of observables including the stellar mass, and UV magnitude (panels b and c in Fig. 5). We find that galaxies with $M_* \gtrsim 10^7 M_\odot$ contribute 20% to the total ionizing photon emissivity in CDM. Given that forthcoming instruments like the JWST will be able to detect galaxies with $M_* \gtrsim 10^{7.5} M_\odot$ (Fig. 4; Dayal et al. 2014b; Pawlik et al. 2011), our results imply that the bulk ($\sim 80\%$) of the stellar mass responsible for producing reionization photons will likely not be directly detectable. As explained above, the contribution to the total ionizing emissivity rises with decreasing m_x , with $M_* \gtrsim 10^7 M_\odot$ galaxies contributing about $\sim 65\%$ to the total for the 2.25 keV model. From the same panel, we see that galaxies with $M_* \gtrsim 10^9 M_\odot$ contribute a negligible 2% to the total emissivity, with this value rising to $\sim 8\%$ in the 2.25 keV model.

Finally, we find that galaxies brighter than $M_{UV} = -13$ provide $\sim 63\%$ of the total ionizing photons for CDM implying that the rest 37% must come from even fainter galaxies. This value rises to about 80% for the 2.25 keV model where fewer lower mass/luminosity halos collapse into bound structures. Currently detected galaxies ($M_{UV} \lesssim -18$) only contribute 6% of the total emissivity in CDM that rises to 18% in the 2.25 keV model with the latter showing a steeper z -evolution of the emissivity driven by the faster galaxy assembly.

To summarize, we find the bulk of the reionization photons come from galaxies with $M_h \lesssim 10^9 M_\odot$, $M_* \lesssim 10^7 M_\odot$ and $-18 \lesssim M_{UV} \lesssim -13$ in CDM. The progressive suppression of low-mass halos with decreasing m_x leads to a shift in the “reionization” population to larger (halo and stellar) masses of $M_h \gtrsim 10^9 M_\odot$ and $M_* \gtrsim 10^7 M_\odot$ for $m_x \gtrsim 3$ keV WDM, although the UV limits effectively remain unchanged.

4 CONCLUSIONS AND DISCUSSION

Although the Cold dark matter (CDM) paradigm has been enormously successful in explaining the large scale structure of the Universe, it shows a number of small scale problems that can be alleviated by invoking (keV) Warm Dark Matter (WDM) particles that erase small scale power, suppressing the formation of low-mass structures. Given that the low-mass high- z galaxies are believed to be the main contributors to the process of cosmic reionization, our aim is to use reionization tracers including the *Planck* CMB electron-scattering optical depth (τ_{es}) and the measured ionizing photon emissivity (\dot{n}_{ion}) to put constraints on the mass (m_x) of WDM particles. We use a merger-tree based semi-analytic model that traces the DM and baryonic assembly of high- z ($z \simeq 5-20$) galaxies in 4 DM cosmologies: CDM and

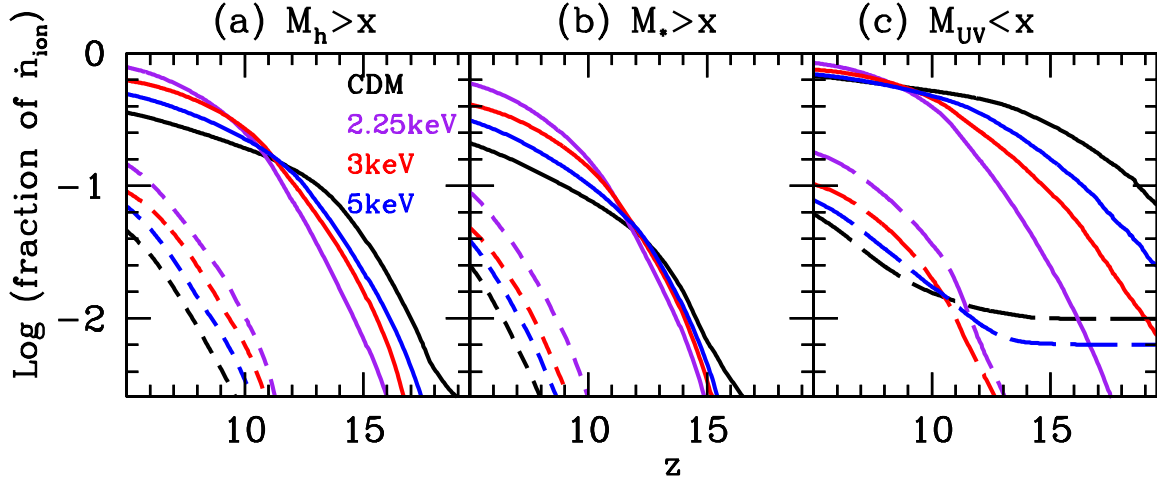


Figure 5. Fractional contribution to the cumulative H I ionizing photon density at $z = 5$ by galaxies of different halo masses (M_h ; left panel), stellar masses (M_* ; middle panel) and UV magnitude bins (M_{UV} ; right panel) for the fiducial DM models considered in this paper, as marked. *Left panel:* the solid and dashed lines show the contribution from galaxies with $x \gtrsim 10^9$ and $10^{10.5} M_\odot$, respectively. *Middle panel:* the solid and dashed lines show the contribution from galaxies with $x \gtrsim 10^7$ and $10^9 M_\odot$, respectively. *Right panel:* the solid and dashed lines show the contribution from galaxies with $x \lesssim -13$ and -18 , respectively.

WDM with $m_x = 2.25, 3$ and 5 keV. Our model includes the key baryonic processes of star formation, SN feedback and the merger/accretion/ejection driven evolution of gas and stellar mass, and has been shown to fit observables over 7 magnitudes (including the UV LFs, M/L ratios and SMD) using only two z and mass-independent free parameters with fiducial values of 3.8% for the maximum star formation efficiency and 10% of the SN energy going into unbinding gas (Dayal et al. 2014a,b). In this work, we use the stellar mass assembly driven ionizing photon output from these theoretical galaxies to model the reionization history. We include the effect of external feedback, i.e., an evolving homogeneous UVB suppressing the baryonic content of galaxies below a threshold mass ($M_h \simeq 10^9 M_\odot$) to explore the WDM masses allowed by reionization constraints. The only additional parameter introduced is the fraction of ionizing photons (f_{esc}) that escape out of galaxies and ionize the IGM.

We find that $m_x \lesssim 2.25$ keV WDM models are ruled out because they yield τ_{es} values lower than that measured by *Planck* even in the (unlikely) case that all the H I ionizing photons produced by every galaxy escape into the IGM (i.e. $f_{esc} = 1$). Thus, using a model that incorporates the key physics driving the baryonic content of high- z galaxies (star formation/feedback/mergers) yields a limit of $m_x \gtrsim 3$ keV that is competitive with results of $m_x \gtrsim 3.3$ keV obtained using the Lyman- α forest (Viel et al. 2013).⁴

We also find that while constant values of $f_{esc} \gtrsim 0.5$ fit the observed τ_{es} for CDM and $m_x \gtrsim 3$ keV WDM, a constant f_{esc} value severely over-predicts the emissivity by about 1.6 (1.9) orders of magnitude for $f_{esc} = 0.2(0.5)$. Rec-

onciling these two data sets requires a z -dependent $f_{esc} = f_0 (\frac{1+z}{7})^\alpha$ which provides enough photons at early times to obtain the right τ_{es} value, whilst yielding low \dot{n}_{ion} values at later times. We find that simultaneously fitting to the two reionization data sets requires $f_0 = (1.65, 1.25, 1.2)\%$ and $\alpha = (5.4, 6.8, 8.2)$ for CDM and $m_x = 5, 3$ keV WDM, respectively. We use the same values for 2.25 keV as for 3 keV since the former never reaches the required τ_{es} value. Quantitatively, we find $f_{esc} \simeq 1.4\%$ at $z \simeq 6$ for all models, rising to 50% at $z \simeq 12, 11, 10$ for CDM, 5 and 3 keV WDM, respectively.

As a result of the presence of the most small-scale structure, reionization starts earliest in CDM, and is 50% complete by $z \simeq 13$. Thereafter, the rising UVB suppresses star formation in the very halos that drive reionization drawing out its end stages. Indeed, reionization is “photon-starved” in CDM and takes a total of about a Gyr to go from a completely neutral to ionized IGM. While the progressive lack of small-scale structure leads to a delay in the start of reionization with decreasing m_x , it also transpires that existing galaxies are less affected by the UVB leading to an enhanced rate in its progress. While the latter effect is dominant for $m_x \gtrsim 3$ keV resulting in reionization lasting for about 780 and 420 Myrs for $m_x = 5$ and 3 keV respectively, reionization lasts for about 580 Myrs in the 2.25 keV model, given its lack of low-mass halos.

Finally, we find that the bulk of H I ionizing photons come from galaxies with $M_h \lesssim 10^9 M_\odot$, $M_* \lesssim 10^7 M_\odot$ and $-18 \lesssim M_{UV} \lesssim -13$ in CDM. The progressive suppression of low-mass halos with decreasing m_x leads to a shift in the “reionization” population to larger (halo and stellar) masses of $M_h \gtrsim 10^9 M_\odot$ and $M_* \gtrsim 10^7 M_\odot$ for $m_x \gtrsim 3$ keV WDM, although the UV limits effectively remain unchanged.

We end with a few caveats. Firstly, we have ignored SN radiative losses that could significantly reduce the to-

⁴ The constraints obtained from reionization models could, however, weaken to $m_x \gtrsim 1.5$ keV in case the bounds on τ_{es} are revised, e.g., as in the latest (12/2014) *Planck* results.

tal energy available to drive winds. However, a decrease in this total energy could be countered by scaling up the fraction of the total energy we put into driving winds from the fiducial value of 10% used in this work. Secondly, Pawlik et al. (2009) have shown that UVB photo-heating reduces the clumping factor of the IGM since the additional pressure support from reionization smoothes out small-scales density fluctuations. While we have used their results for an overdensity of 100, we have confirmed that our results do not change using threshold values of 50, or 200. Thirdly, while we assume that all halos with mass $M_h \lesssim 10^9 M_\odot$ are feedback suppressed, we find our results are equally consistent with observations (τ_{es} and \dot{n}_{ion}) using values ranging between $10^{8.5} - 10^{9.5} M_\odot$. Finally, we have made the simplifying assumption of using a mass-independent f_{esc} at all z . This is partly motivated by the uncertainty regarding the mass-dependence of f_{esc} : while some authors find f_{esc} to decrease with an increase in the halo mass (Razoumov & Sommer-Larsen 2010; Yajima et al. 2011; Ferrara & Loeb 2013), other works have found the opposite trend (Gnedin et al. 2008; Wise & Cen 2009). Although there are a number of caveats involved, our model fits observed UV LFs at faint end validating the theoretical underlying stellar population. Unless the results on LBG faint-end or τ_{es} evolve significantly, our results rule out $m_x \lesssim 2.25$ keV WDM models. Significant progress is expected to be made by comparing our model predictions with actual faint LBG data such as that imminently expected from the Frontier Fields, and from forthcoming observatories such as the *JWST*. Furthermore, if the claim of 3.5 KeV X-ray line holds to be true, it will usher in an exciting era for WDM dominated cosmology.

ACKNOWLEDGMENTS

PD acknowledges the support of the Addison Wheeler Fellowship awarded by the Institute of Advanced Studies at Durham University and of the European Research Council. VB acknowledges support from NSF grant AST-1413501. The authors thank A. Taylor, M. Viel for helpful discussions and A. Mazumdar for help with understanding the particle physics behind WDM.

REFERENCES

Abazajian K., Acero M., Agarwalla S., Aguilar-Arevalo A., Albright C., et al., 2012
Barkana R., Haiman Z., Ostriker J. P., 2001, *ApJ*, 558, 482
Barkana R., Loeb A., 2001, *Phys. Rep.*, 349, 125
Benson A. J. et al., 2013, *MNRAS*, 428, 1774
Blumenthal G. R., Faber S. M., Primack J. R., Rees M. J., 1984, *Nature*, 311, 517
Bode P., Ostriker J. P., Turok N., 2001, *ApJ*, 556, 93
Bolton J. S., Haehnelt M. G., 2007, *MNRAS*, 382, 325
Bond J. R., Szalay A. S., 1983, *ApJ*, 274, 443
Bouwens R. J. et al., 2010, *ApJ*, 725, 1587
Bouwens R. J. et al., 2011, *ApJ*, 737, 90
Bouwens R. J. et al., 2014, *ArXiv:1403.4295*

Bowler R. A. A. et al., 2014a, *ArXiv e-prints*
Bowler R. A. A. et al., 2014b, *MNRAS*, 440, 2810
Boyarsky A., Ruchayskiy O., Iakubovskiy D., Franse J., 2014, *Phys.Rev.Lett.*, 113, 251301
Boylan-Kolchin M., Bullock J. S., Kaplinghat M., 2012, *MNRAS*, 422, 1203
Bradley L. D. et al., 2012, *ApJ*, 760, 108
Bromm V., Yoshida N., 2011, *ARA&A*, 49, 373
Bulbul E., Markevitch M., Foster A., Smith R. K., Loewenstein M., et al., 2014, *Astrophys.J.*, 789, 13
Calura F., Menci N., Gallazzi A., 2014, *MNRAS*, 440, 2066
Castellano M. et al., 2010, *A&A*, 524, A28
Choudhury T. R., Ferrara A., 2005, *MNRAS*, 361, 577
Choudhury T. R., Ferrara A., 2006, *MNRAS*, 371, L55
Choudhury T. R., Ferrara A., 2007, *MNRAS*, 380, L6
Choudhury T. R., Ferrara A., Gallerani S., 2008, *MNRAS*, 385, L58
Ciardi B., Ferrara A., 2005, *Space Sci. Rev.*, 116, 625
Cole S. et al., 2005, *MNRAS*, 362, 505
Dayal P., Ferrara A., Dunlop J. S., Pacucci F., 2014a, *MNRAS*, 445, 2545
Dayal P., Mesinger A., Pacucci F., 2014b, *ArXiv:1408.1102*
de Souza R. S., Mesinger A., Ferrara A., Haiman Z., Perna R., Yoshida N., 2013, *MNRAS*, 432, 3218
de Vega H. J., Sanchez N. G., 2010, *MNRAS*, 404, 885
Ferrara A., Loeb A., 2013, *MNRAS*, 431, 2826
Gnedin N. Y., Kravtsov A. V., Chen H.-W., 2008, *ApJ*, 672, 765
Governato F. et al., 2014, *ArXiv e-prints*
Haardt F., Madau P., 2012, *ApJ*, 746, 125
Hinshaw G. et al., 2013, *ApJS*, 208, 19
Kang X., Macciò A. V., Dutton A. A., 2013, *ApJ*, 767, 22
Klypin A., Kravtsov A. V., Valenzuela O., Prada F., 1999, *ApJ*, 522, 82
Kuhlen M., Faucher-Giguere C.-A., 2012, *MNRAS*, 423, 862
Lange A. E. et al., 2001, *Phys. Rev. D*, 63, 042001
Leitherer C. et al., 1999, *ApJS*, 123, 3
Macciò A. V., Paduroiu S., Anderhalden D., Schneider A., Moore B., 2012, *MNRAS*, 424, 1105
McLure R. J. et al., 2013, *MNRAS*, 432, 2696
McLure R. J., Dunlop J. S., Cirasuolo M., Koekemoer A. M., Sabbi E., Stark D. P., Targett T. A., Ellis R. S., 2010, *MNRAS*, 403, 960
Mitra S., Choudhury T. R., Ferrara A., 2011, *MNRAS*, 413, 1569
Mitra S., Choudhury T. R., Ferrara A., 2012, *MNRAS*, 419, 1480
Moore B., Quinn T., Governato F., Stadel J., Lake G., 1999, *MNRAS*, 310, 1147
Navarro J. F., Frenk C. S., White S. D. M., 1997, *ApJ*, 490, 493
Oesch P. A. et al., 2010, *ApJ*, 709, L16
Oesch P. A. et al., 2013, *ApJ*, 773, 75
Pacucci F., Mesinger A., Haiman Z., 2013, *MNRAS*, 435, L53
Parkinson H., Cole S., Helly J., 2008, *MNRAS*, 383, 557
Pawlik A. H., Milosavljević M., Bromm V., 2011, *ApJ*, 731, 54

- Pawlik A. H., Schaye J., van Scherpenzeel E., 2009, MNRAS, 394, 1812
- Peebles P. J. E., 1971, *Physical cosmology*
- Planck Collaboration et al., 2014a, A&A, 571, A1
- Planck Collaboration et al., 2014b, A&A, 571, A16
- Razoumov A. O., Sommer-Larsen J., 2010, ApJ, 710, 1239
- Schneider A., Anderhalden D., Macciò A. V., Diemand J., 2014, MNRAS, 441, L6
- Schultz C., Oñorbe J., Abazajian K. N., Bullock J. S., 2014, ArXiv:1401.3769
- Sheth R. K., Tormen G., 1999, MNRAS, 308, 119
- Slosar A. et al., 2013, J. Cosmology Astropart. Phys., 4, 26
- Somerville R. S., 2002, ApJ, 572, L23
- Songaila A., Cowie L. L., 2010, ApJ, 721, 1448
- Subramanian K., Cen R., Ostriker J. P., 2000, ApJ, 538, 528
- Teyssier R., Pontzen A., Dubois Y., Read J. I., 2013, MNRAS, 429, 3068
- Viel M., Becker G. D., Bolton J. S., Haehnelt M. G., 2013, Phys. Rev. D, 88, 043502
- Viel M., Lesgourgues J., Haehnelt M. G., Matarrese S., Riotto A., 2005, Phys. Rev. D, 71, 063534
- Weinberg D. H., Bullock J. S., Governato F., Kuzio de Naray R., Peter A. H. G., 2013, ArXiv e-prints
- Wise J. H., Cen R., 2009, ApJ, 693, 984
- Wyithe J. S. B., Bolton J. S., 2011, MNRAS, 412, 1926
- Wyse R. F. G., 2001, in *Astronomical Society of the Pacific Conference Series*, Vol. 230, *Galaxy Disks and Disk Galaxies*, Funes J. G., Corsini E. M., eds., pp. 71–80
- Yajima H., Choi J.-H., Nagamine K., 2011, MNRAS, 412, 411